Research Signpost
37/661 (2), Fort P.O., Trivandrum-695 023, Kerala, India

Photonic Glasses, 2006: ISBN: 81-308-0063-2 Editor: Rolindes Balda

4 Sol-gel derived photonic bandgap structures

Rui M. Almeida and M. Clara Gonçalves
Departamento de Engenharia de Materiais/ICEMS, Instituto Superior Técnico
Av. Rovisco Pais, 1049-001 Lisboa, Portugal

Abstract

Photonic bandgap (PBG) structures, or photonic crystals (PCs), form a promising new class of optical materials with an enormous potential for fundamental science and applications, including the localization of light at defects and surfaces and the inhibition of the emission of radiation. In recent years, several artificial dielectric structures have been found to possess a photonic band gap. This article provides an overview of 1-D and 3-D PBG, glass-based and other dielectric structures, fabricated based on sol-gel processing.

Correspondence/Reprint request: Dr. Rui M. Almeida, Departamento de Engenharia de Materiais/ICEMS Instituto Superior Técnico, Av. Rovisco Pais, 1049-001 Lisboa, Portugal. E-mail: rui.almeida@ist.utl.pt

Nomenclature

1-D	One-dimensional
2-D	Two-dimensional
3-D	Three-dimensional
DBR	Distributed Bragg reflector
FWHM	Full-width at half-maximum
IR	Infrared
f	filling ratio
fcc	Face-centred cubic
LED	Light emitting diode
PBG	Photonic bandgap
PC	Photonic crystal
PL	Photoluminescence
PMMA	Polymethyl methacrylate
PS	Polystyrene
RE	Rare-earth
RGB	Red/Green/Blue (colour system)
RI	Refractive index
VLSI	Very large scale integration
SEM	Scanning Electron Microscopy
sc	simple cubic

1. Introduction

In nature, many colours cannot be explained simply by the absorption and reflection of light, but arise from physical mechanisms such as light scattering, interference and diffraction from ordered structures with periodicities in the submicron range. Wings of butterflies [1], peacock feathers, bat stars, fish scales, precious opals [2], or the multilayered structure of pearls, are examples of such natural structures. Compact disks are synthetic structures with the same optical characteristics. The iridiscent colours of these materials show angle dependence, determined by the periodic structure of each material; in addition to strong multiple scattering of light, unexpected forbidden wave propagation in certain frequency ranges of normally transparent materials is observed.

Near the end of the twentieth century, E. Yablonovich [3] and S. John [4] proposed the idea that an artificial structure with a periodic modulation in refractive index (RI) (or dielectric constant) can prevent the propagation of light over a certain band of wavelengths, where the isolated materials are otherwise transparent, while allowing other bands to propagate. The periodicity prevents light from propagating through the material due to Bragg reflection, in a wavelength range of the order of the spatial period of

the PBG structure, or simply, PC. When the RI periodicity is on a millimetre scale, the PBG confines and controls the light in the microwave regime [5, 6], while in the infrared (IR) scale the PBG does the same in the optical regime [7, 8]; when the periodicity is of the order of a few angstroms, the PBG operates in the X-ray regime, thus being a common solid-state crystal formed by atoms, ions or molecules. Such materials exhibit thus PBGs, analogous to the electronic bandgaps for Bloch electron waves in semiconductors and their transmission at certain well-defined frequencies is dictated by the periodicity, direction of propagation and polarization of light. However, devices for near-IR and optical frequencies present challenges, both for adequate micro-fabrication techniques and selection of materials with sufficiently high RI contrast.

Depending up on the dimensionality of the periodicity, one can have PCs in one (1-D), two (2-D) or three dimensions (3-D) (Figure 1). A complete PBG, where all electromagnetic propagation is disallowed whatever the direction of propagation or the polarization, for a certain range of frequencies, is only possible in 3-D structures. In the case of sol-gel derived materials [9], the main emphasis has been on 1-D and 3-D structures [10-13 and references wherein].

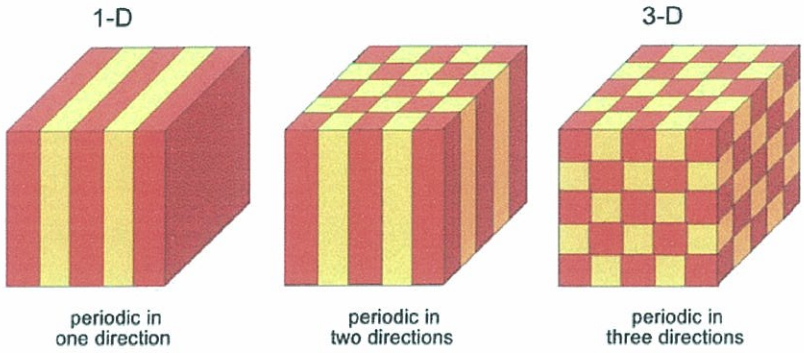

Figure 1. 1-D, 2-D and 3-D photonic crystals.

An important quantum-optical consequence is that spontaneous emission of excited atoms or molecules inside the PC is completely inhibited. Moreover, controlled defects in a PC will result in localized states in the bandgap, as if light were trapped in a cage [14-19]. Thus, it is believed that PCs should be able to transfer the full functionality of semiconductor devices into the all-optical field, combining high integration and high speed processing. The potential applications of PCs are highly prospective, ranging from high-performance LEDs, low-power microlasers and novel types of optical fibers, to high-speed switches, optical filters and photonic very large scale integration (VLSI) [20].

2. Photonic crystals – How they work

The physical phenomenon which describes the PBG behaviour is the localization of light, which is achieved from the scattering and interference produced by a coherent wave in a periodic structure. The periodicity of the PC structure has thus to be in the same length scale as the wavelength of the electromagnetic waves, i.e., ~ 300 nm for PCs operating in the visible part of the spectrum. When white light shines upon the PC, certain wavelengths do not penetrate very far and are selectively reflected from the periodic scatterers of the PC, like the highest density plane (111) in a face-centred cubic (*fcc*) structure (Figure 2). Each wavelength is reflected exactly at the same frequency as the incident light, regardless of its direction or polarization state, for a full PBG structure. Then, wherever in space the radiation interferes constructively, by adding scattered rays with phase differences multiple of 2π, a coloured crystal will be observed. The wavelength (or frequency) range which is forbidden to propagate through the periodic structure is called a *stop band* and corresponds to a *photonic bandgap* in the optical density of states. The remaining transmitted light generates the complementary colour.

By analogy with X-ray diffraction, the interaction of white light with the PC is described by the modified form of Bragg's law for the optical region, which takes into account Snell's law of refraction [21]:

$$\lambda = 2d\sqrt{n_{eff}^2 - \sin^2\theta} \tag{1}$$

where λ is the free space wavelength of the light, d the interplanar spacing between the scattering planes, θ is the angle between the incident radiation and the normal to the set of planes and n^2_{eff} is the effective dielectric constant of the composite PC (Figure 2). Since the (111) plane is the most densely packed in the *fcc* arrangement, with spacing $d_{hkl} = \frac{a}{\sqrt{h^2+k^2+l^2}}$ and $d_{(111)} = \frac{a}{\sqrt{3}}$, where $a = \frac{2D}{\sqrt{2}}$ and D is the sphere diameter in a colloidal PC, the longest wavelength diffracted by the *fcc*-packing, for an observer perpendicular to the surface, will be:

$$\lambda_{max} = 2n_{eff}\frac{D\sqrt{2}}{\sqrt{3}} = 1.633 n_{eff} D \tag{2}$$

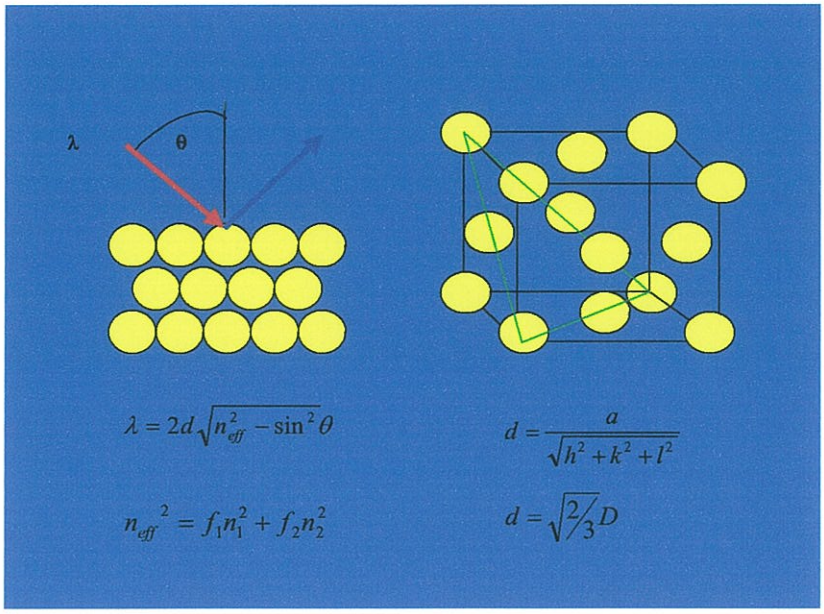

Figure 2. Diffraction of white light by *fcc* colloidal crystals at the (111) crystal planes. The (111) crystal plane is the most densely packed in the *fcc* arrangement, with a spacing $d_{(111)}$, related to the sphere diameter, D. (Adapted from Ref. [22]).

The diameter of the spheres is comparable to the wavelength of visible light, so the *opal* acts as a 3-D diffraction lattice for visible light and its colours are determined by the diameter of the spheres and the RI of the composite.

3. Photonic bandgap structures – Electromagnetic localization in photonic crystals

As in semiconductor physics, by introducing specific defects (point, line and/or planar) into PBG structures, states in the gap with localized wavefunctions are created. A defect in an otherwise perfect periodic structure can allow light to be trapped in the vicinity of the defect, while being excluded from the medium surrounding it. Adding or removing a certain amount of dielectric material from the PC disrupts the symmetry of the photonic lattice and the flow of photons inside can then be manipulated, allowing either a single state, or multiple closely separated states, to exist within the bandgap. Therefore, many efforts have been devoted to the creation of PCs with specific band structures [5, 14, 16-19]. However, if the defects are randomly distributed, the optical response is given by the average of all defect configurations, resulting in a decrease of the Bragg peak intensity [23].

The existence of localized states, due to the introduction of point defects, can be useful in designing high-Q value microcavities in PCs (Figure 3). When line defects are introduced into a PBG lattice, an electromagnetic wave with a frequency within the bandgap of the structure can be guided through the crystal.

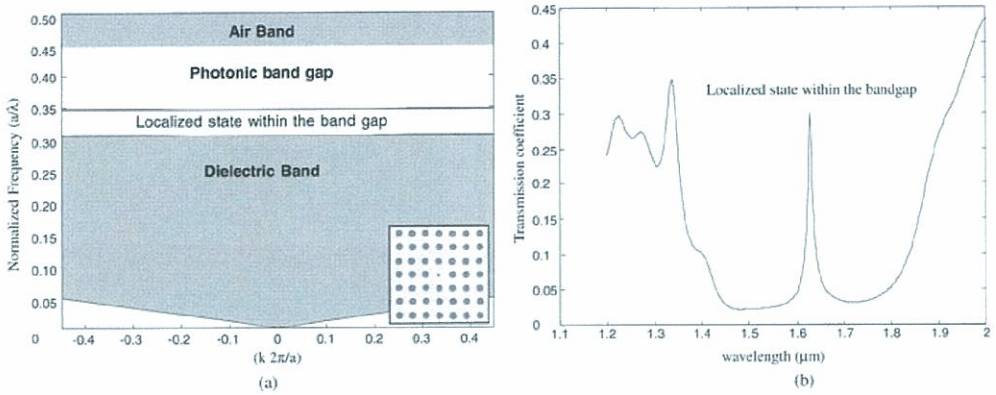

Figure 3. Photonic crystals with designed defects: a point defect, which will allow a single localized mode to exist in the bandgap. (Reproduced with permission from Ref. [24]).

4. Optical characterization

The main techniques for characterization of PBG materials are optical. Optical reflectance and transmission are the principal tools used to characterize 3-D systems [25, 26]. In a reflectance experiment, a high symmetry facet of the PBG is often chosen [27]. For transmission, the detector is placed in line behind the sample, and Bragg reflected photons are recorded as drops in transmitted intensity. At variance with the specular reflectance geometry, the transmission experiment does not select a Bragg plane because it does not rely on detecting the scattered photon but instead on detecting its absence. In both approaches, the optical properties may contain spatially averaged contributions of many different emitters.

5. Photonic crystals – Fabrication methods and resulting structures

For near-IR frequencies, self-assembly techniques offer many potential advantages in opal and inverse opal fabrication. Compared to competing techniques involving micromanipulation [28], layer-by-layer growth [7, 29-34], lithography and selective etching techniques [29, 35-37], or 3-D holography by means of multiple laser beams [38-42], self-assembly

[8, 17, 43-63] is significantly less costly and it is compatible with VLSI technologies. In addition, self-assembly techniques offer an impressive versatility with respect to the materials used in fabricating the crystals. Unfortunately, self-assembly methods lead only to a few crystalline structures, since *fcc* or *sc* structures of touching spheres are most often the result (Figure 4).

The process of colloidal crystallization has been extensively studied, leading to the development of several methods to prepare high quality colloidal crystals with few crystalline defects. These techniques include electrostatically induced crystallization [43-47], gravity sedimentation [17, 48-50], electro-hydrodynamic deposition [51-54], colloidal epitaxy [55], physical confinement [56, 57], centrifugation [58] and vertical convective self-assembly [8, 59-63].

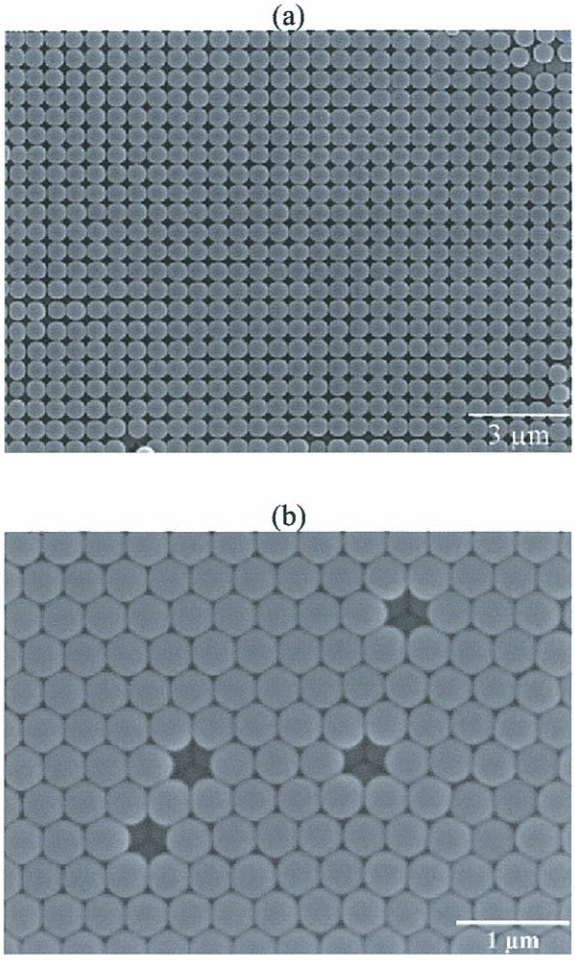

Figure 4. SEM micrographs of opals made of 460 nm diameter PS spheres, showing: (a) *sc* and (b) *fcc* structures.

5.1. 1-D PBG structures

5.1.1. Bragg reflectors

1-D structures have probably been the most developed by sol-gel processing. Distributed Bragg reflectors (DBRs), or Bragg mirrors, are the most studied 1-D sol-gel structures. Their overall reflectivity, which can be higher than that of metallic mirrors, is due to Bragg (not Fresnel) reflection (equation (*1*)). 1-D PBG structures usually consist of a stack of dielectric layers with alternating high and low refractive indices. The optical thickness, *nx*, of each layer equals $\lambda/4$, λ being the wavelength for which Bragg reflection occurs, *n* the RI of the material and *x* the layer thickness. Higher index layers, therefore, will have lower physical thickness, *x*, so that the optical thickness is the same for all layers.

Sol-gel DBRs are usually made by dip-coating [64-67], or spin-coating [12, 13, 68-71]. The RI contrast and the number of layers are the most important parameters. SiO_2, TiO_2 and ZrO_2 are often chosen, due to the differences in their RIs. The higher the RI contrast and the larger the number of layers, the higher is the reflectivity of the stop-band. However, the larger the number of layers, the higher is the risk of craks developing. To overcome this drawback, short densification heat treatments at high temperatures should be used [12, 67].

5.1.2. Microcavities

The controlled introduction of defects leads to some interesting 1-D PBG applications. One example is the Fabry-Perot microcavity [12, 13, 66, 67], which may be achieved by the introduction of an extra layer, or the suppression of a layer, within a multilayer stack (Figure 5).

The reflectance minimum corresponding to the microcavity resonance (or *pass band*) inside the stop band appears at $\lambda = 2nx$. The quality factor of a microcavity is given by:

$$Q = \frac{\lambda}{\Delta\lambda} \tag{6}$$

where λ is the resonance wavelength and $\Delta\lambda$ is the cavity full width at half maximum (FWHM).

5.2. 2-D PBG structures

2-D structures, either planar or in fiber form, have been found difficult to fabricate by sol-gel processing and they will not be considered in this review.

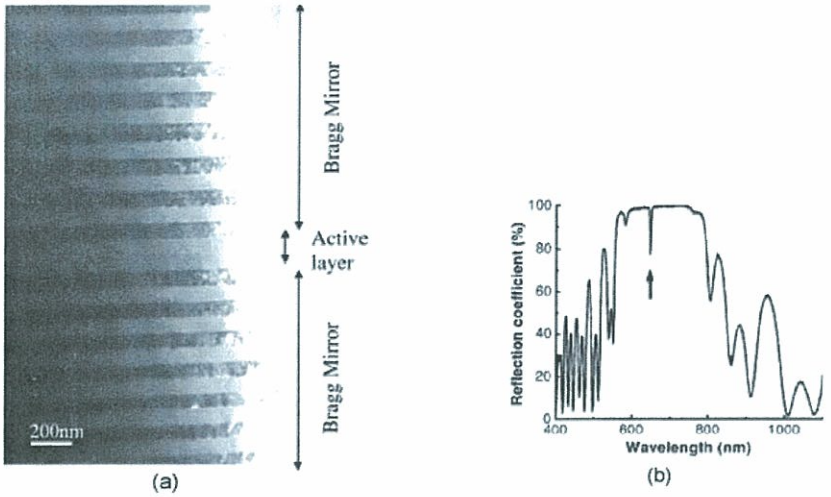

Figure 5. (a) Cross section transmission electron micrograph of a Fabry-Perot microcavity, consisting of alternating SiO_2 (bright) and TiO_2 (dark) quarter-wave layers, with a half-wave (defect) cavity layer of SiO_2. (b) reflection spectrum of the microcavity, with a stop band extending from 580 to 780 nm and a resonance minimum at 649 nm. (Reproduced with permission from ref. [66]).

5.3. 3-D PBG structures

5.3.1. Vertical convective self-assembly – The simplest way to fabricate a 3-D photonic crystal

Precious opal is a natural iridescent material. In the gem opal, nature spontaneously makes simple *fcc* crystals, where amorphous SiO_2 spheres naturally self-assemble in regular *fcc* globules, cemented by a disordered matrix of silica spheres and amorphous silica [2]. The amorphous silica spheres are ordered like the atoms in a crystal lattice, but on a scale a thousand times larger.

To mimic these natural opal crystals is thus an experimental route to achieve PBG materials. Vertical convective self-assembly deposition [8, 59-63] is achieved with a substrate placed vertically into a vial containing a colloidal suspension. Colloidal spheres of, for example, SiO_2, TiO_2, polystyrene (PS), poly(methyl methacrylate) (PMMA) etc., owing to their mainly isotropic electrostactic interaction, can self-organize into crystalline lattices when the volume fraction reaches a certain value. As the solvent evaporates and the meniscus is swept downwards, the colloidal particles self-assemble on the surface of the vertical substrate (Figure 6). To the unaided eye, optical Bragg reflections of air-sphere crystals deposited on the substrate appear as coloured reflections. By adjusting the volume fraction, the thickness of the resulting deposit can be controlled (Figure 7). Self-organization by convective self-assembly, besides resulting always in polycrystalline materials, has a processing time which is quite long (within ~ 3-5 weeks).

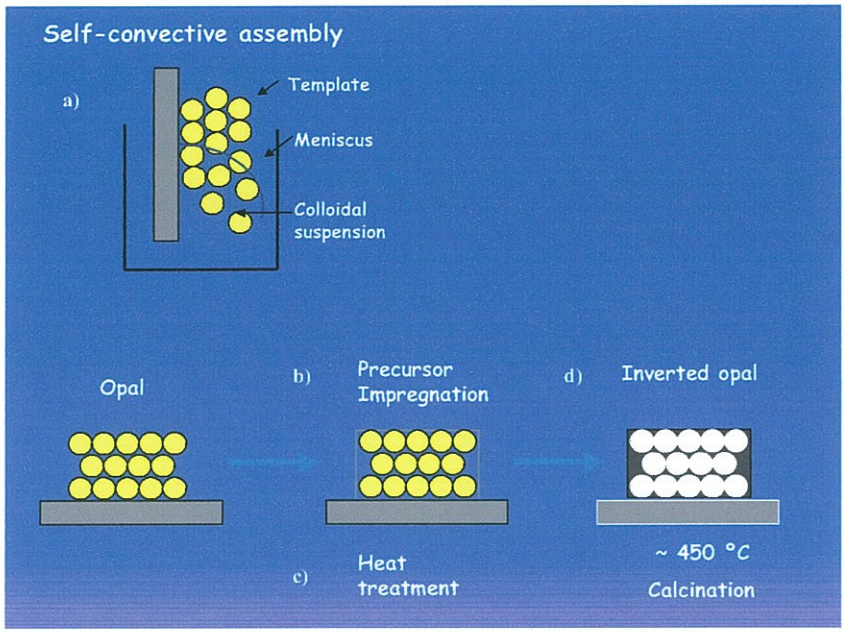

Figure 6. Fabrication of an inverted opal by convective self-assembly: a) colloidal particles are forced into an ordered arrangement on the surface of a vertical substrate, as the meniscus is swept downwards by evaporation of the solvent; b) once the template is formed, the voids of the opal are uniformly infiltrated with a higher RI material through a sol-gel process; c) a heat treatment is performed in order to achieve a solid structure from the sol-gel precursors; d) finally, the inverse-opal crystal (the negative of an opal structure) is obtained by removing the original template material by calcination (for PS or PMMA), or etching in hydrofluoric acid (for silica colloids). (Adapted from Ref. [73]).

(a) (b)

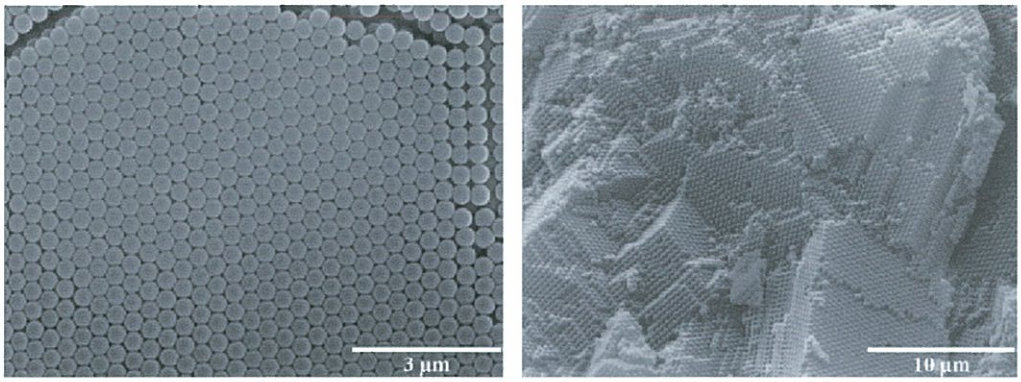

Figure 7. SEM micrograph of a typical opal made of 460 nm diameter PS spheres prepared by self-convective assembly: (a) top view; (b) cleaved edge showing different crystalline planes, {100} and {111}, of the *fcc* structure.

`The natural opal structures have the right size for the optical range, but, unfortunately, a small RI variation. Thus, infiltration by a dielectric material of high RI, or a semiconductor, plus removal of the original template by wet etching or calcinations, enhances the PBG behaviour of the matrix (Figure 8). Semiconductor infilling, e.g. with InP or CdS, can be used in order to either enhance the PBG properties, or to inhibit spontaneous emission of the guest, or both [72]. Judicious choice of opal sphere size and semiconductor content allow the matching of the photonic gap of the opal to the semiconductor emission, such that the PBG effects of the host can be best observed.

New possibilities emerge when the substrate has been previously micro-patterned. Based on the wide range of soft lithography possibilities, a multitude of structures with different shapes and architectures can be fabricated.

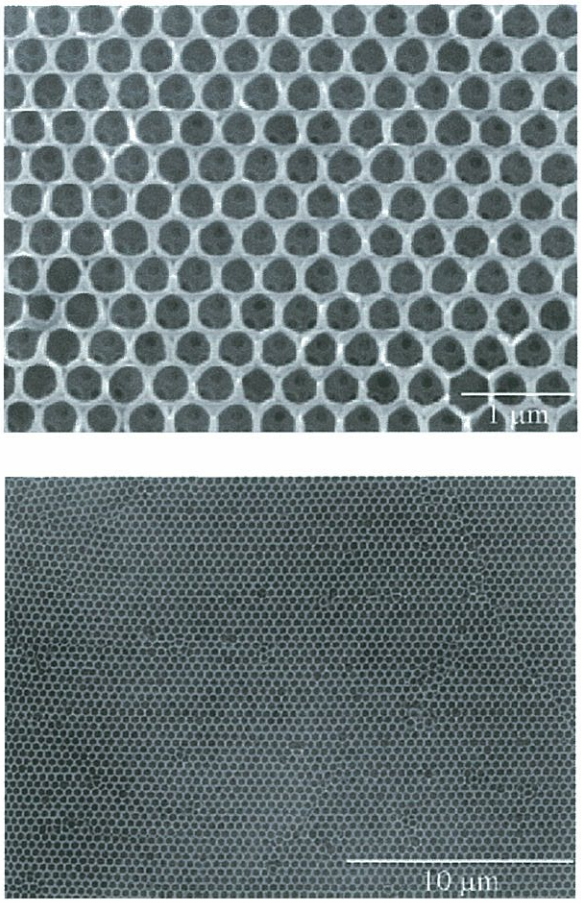

Figure 8. SEM micrograph of titania/air inverted opal structure, prepared from self-convective assembled PS templates at two different magnifications.

5.3.2. DIP-coating – A quicker way to fabricate a 3-D photonic crystal

For colloidal crystal growth by dip-coating [11], a glass slide is vertically immersed into the aqueous colloidal suspension, it is left standing for some minutes while the colloidal spheres are allowed to stick onto it and it is then withdrawn at low speed. Thicker films are fabricated by successive dips. An example is shown in Figure 9, where an iridescent array of PS spheres remained on the glass substrate, revealing a well organized nanostructure. Infiltration and template removal were the subsequent steps.

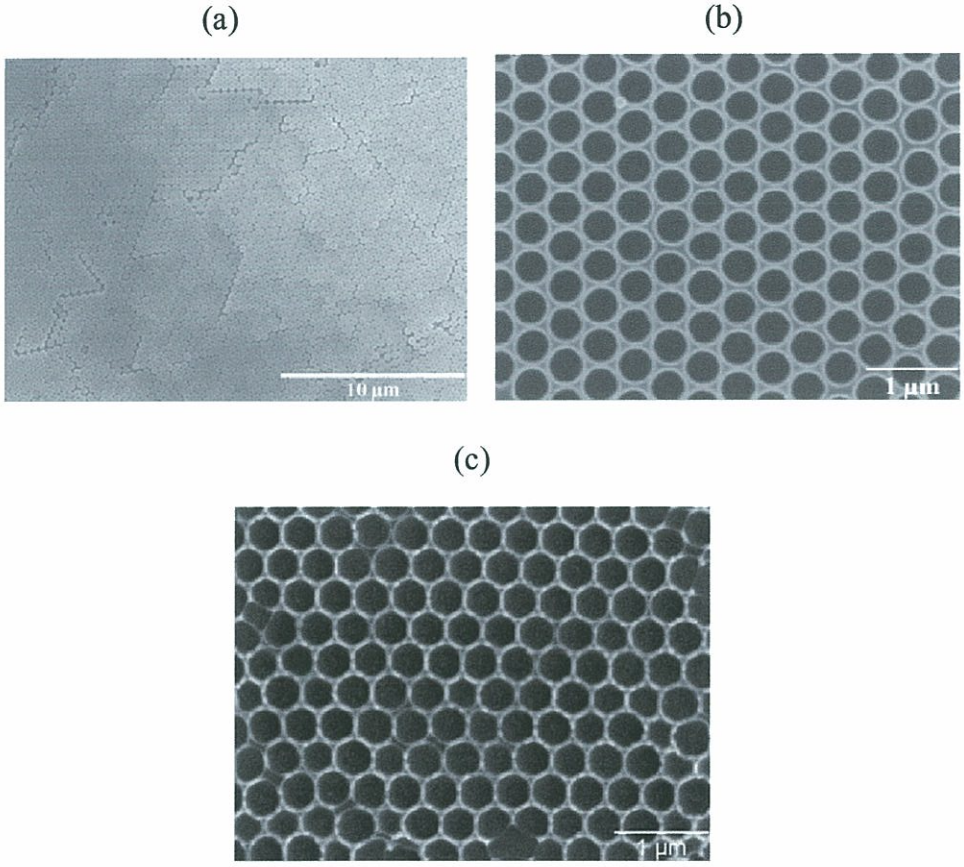

Figure 9. SEM micrographs of colloidal crystals made from 460 nm PS spheres, prepared by dip-coating: (a) PS opal structure; (b) titania infiltrated PS template; (c) inverse opal, consisting of air spheres in a titania matrix.

A so modified coating method has been tested in our laboratory. Before the first dip and after wetting the substrate with a low surface tension liquid ($\gamma_{ethanol} = 22.8\ mNm^{-1}$) [74], a drop of the colloidal suspension ($\gamma_{water} = 72.75\ mNm^{-1}$) [74] is placed on the liquid film. Defining the spreading coefficient, S, as:

$$S = \gamma_{sv} - (\gamma_{sl} + \gamma_{lv}) \quad (7)$$

where γ_{sv}, γ_{sl}, γ_{lv} are the surface tensions of the phases in contact involved, natural spreading will occur for positive S values [75]. In the present case, the initial spreading coefficient is S = 16.76 mNm^{-1} ($\gamma_{ethanol/34\%water}$ = 33.24 mNm^{-1}) [74] and the suspension spontaneously spreads as a thin film on ethanol, allowing self-assembly of the spheres. Larger organized areas are produced with this technique.

5.3.3. Sedimentation – The natural way to obtain opals

Sedimentation is the natural way to obtain precious opals. In practice, a sphere suspension is left to settle over a horizontal substrate, where sedimentation is obtained, driven by gravity [17, 48-50]. The water in excess is removed, while avoiding disturbances in the sediment; at this stage, the residual water content in the opal is about 10 wt %. The sediment is then dried and heat treated. The final product is a compact of spheres arranged in a *fcc* structure (Figure 10), whose photonic properties scale with the sphere diameter (Figure 11). For low colloidal concentrations (~1 wt%), the sphere size can be accurately determined from Stokes'law [17], if the density and viscosity are known.

Although the self-organization of the colloid results in a crystalline structure, the processing time is long, running from a few days to several weeks, depending on the colloid size.

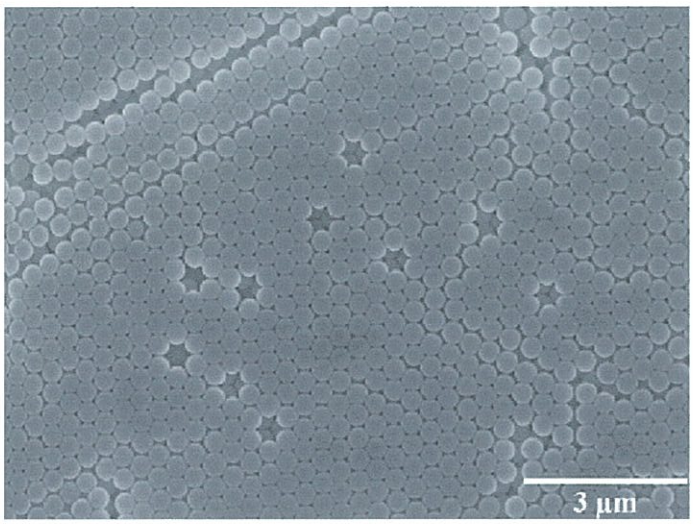

Figure 10. SEM micrograph of an opal structure made from 460 nm PS spheres, prepared by sedimentation.

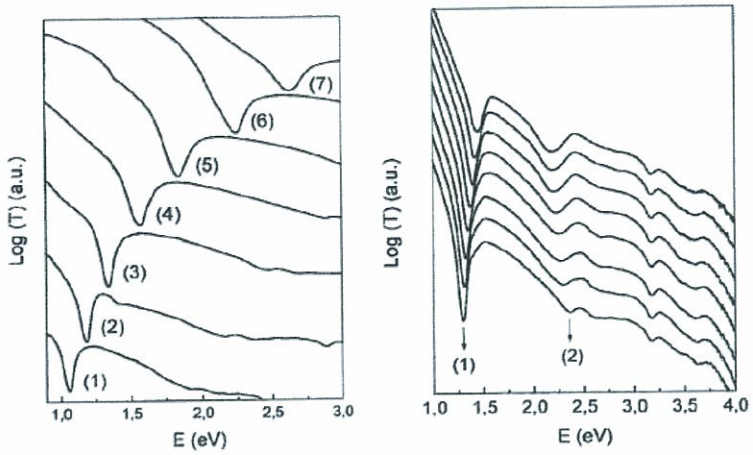

Figure 11. (a) Optical transmission at normal incidence (θ= 0°) for opal-like structures made of spheres with different diameters: (1) 535 nm, (2) 480 nm, (3) 415 nm, (4) 350 nm, (5) 305 nm, (6) 245 nm, and (7) 220 nm. The spectra have been vertically shifted for the sake of clarity. (Reproduced with permission from ref. [76]).

6. The presence of defects

6.1 Random defects

The main problem found in the preparation of opals and inverted opals is the unavoidable presence of defects due both to the dispersion in the microsphere diameters and the common stacking defects developed during crystal growth. In practice, non-uniformities occur at every step of the fabrication process. For instance, some spheres may not sit at exact lattice sites when they form colloidal crystals. When infiltration takes place, sol-gel reactions can be incomplete. Drying invariably involves a crystal contraction, which is not accompanied by the supporting substrate and which can only be accommodated by the production of cracks. Inverse opals, being a replica of the self-assembled crystal template, will reproduce the same type of defects. Further, in a latter step of the inverse opal fabrication, the removal of the template can be incomplete. To overtake this drawback, for example, an emulsion of oil in formamide has been used as a template [77]. Oil droplets are highly deformable, allowing the precursor solution to accommodate large shrinkage and avoiding cracks.

The optical spectra will reveal all these features as broadening of the peaks, diffuse scattering and a decrease in reflectance at the gap frequency [78]. It has been demonstrated, by means of numerical simulations, that the bandgap is strongly affected by geometrical disorder, such as variations in the radii of the spheres (size randomness) and random displacements of the spheres from lattice sites (site randomness). At a disorder magnitude

smaller than two percent of the lattice constant, the bandgap can be closed, even in the presence of a very high RI contrast [79, 80].

6.2. Engineered defects

When PCs are formed via lithography or micromachining, point, linear or planar defects naturally can also be built into the structure during the fabrication process. However, in the case of self-assembled crystals, the fabrication of particular types of defects in specific locations within the periodic lattice is not straightforward. Nevertheless, much work on the incorporation of specific types of structural defects into 3-D colloidal crystals has been performed [81-84]. One way of introducing structural disorder in artificial opals is by adding controlled amounts of dopant spheres different from those of the host. Either by increasing the dopant sphere concentration [83, 85], or by increasing the size of the defect [83] while keeping its concentration constant, a decrease in the Bragg peak is attained, proving that structural disorder in PCs increases with the dopant concentration in the host matrix.

The modification of a synthetic opal just after self-assembly could be another strategy to build specific defects into a PC. First, the empty space in the opal may be filled with a monomeric substance which can be polymerised by the action of multiple incident photons; secondly, a confocal microscope may be used to focus a laser beam at precise positions inside the structure. Because multiphoton polymerisation depends exponentially on the intensity of the laser light, polymerisation occurs only within a very small volume at the focal point of the microscope. As the laser focus is moved, 3-D defects of any desired shape can be written inside the template. After polymerisation, the unexposed monomer is dissolved away, leaving behind photogenerated patterns within the inverted opal [83].

A patterned substrate can also be used in order to obtain engineered defects. This technique can be combined with others in order to attain thickness and orientation control at the same time; therefore, crystallization is directed to take place according to a predefined geometry, giving rise to a template-directed sedimentation [86], or a patterned confinement cell [87].

7. Photonic crystal applications

7.1. Photoluminescence

Dopant species may be included in the liquid phase, during sol-gel fabrication. Eu^{3+}-doped microcavities have been produced by adding $Eu(NO_3)_3$ to the precursor solution [66, 67]. The cavity was formed by a half-wave Eu^{3+}-doped SiO_2 layer inserted between two DBRs, consisting of

seven pairs of quarter-wave, alternating high/low index layers. The Eu^{3+} luminescence at ~ 615 nm ($^5D_0 \rightarrow {}^7F_2$ transition) has a line shape which was strongly modified in the cavity and its intensity was enhanced (by a factor of ~20) for the wavelength corresponding to the cavity resonance, whereas it was weakened for the other emission wavelengths.

On the other hand, erbium/ytterbium-doped 1-D PBG structures have also been prepared by sol-gel [88]. 1-D coupled Fabry-Perot microcavities showed efficient energy transfer at 980 nm from Yb^{3+} to Er^{3+} ions, and efficient Er^{3+} photoluminescence (PL) at ~ 1.5 μm, as long as the two types of ions were present simultaneously in the same defect layer [88] (Figure 12).

Other recent studies have been devoted to luminescent materials infiltrated into opal [89] and inverted opal [90, 91] matrices. A successful attempt to combine ZnO with a PC has been achieved for a 3-D periodic structure, by growing ZnO inside a PC in the solution containing a zinc nitrate or zinc acetate precursor. The PL spectra of the ZnO powder exhibited very high and broad emission peaks in the green region, due to crystal defects such as oxygen vacancies and zinc ion interstitials. In contrast to the PL spectra of ZnO powder, nanocrystals of ZnO embedded into the voids of an *fcc* opal matrix exhibited a dominant ultraviolet plus a rapidly decreasing green PL emissions with decreasing temperature. These results indicate that the luminescent materials embedded into PCs are promising for the fabrication of RGB pixels in full-color displays.

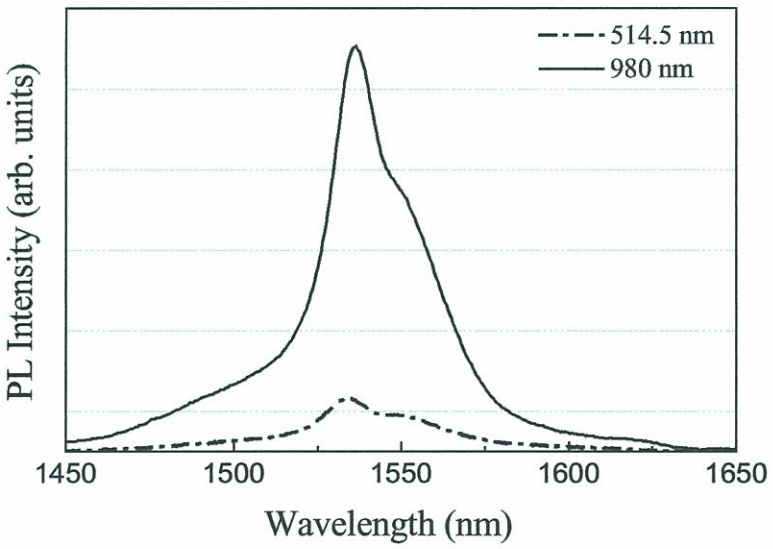

Figure 12. Comparison of Er^{3+} photoluminescence spectra of coupled microcavity A, excited at 514.5 nm and 980 nm, at normal incidence.

Zinc sulphide (ZnS) can be used in PCs due to its high RI and large electronic bandgap, which make it highly transparent in the visible and near IR regions. ZnS has been infiltrated by a sol-gel technique within opal templates and it was heterogeneously nucleated and grown [92]. The stop band could be easily taylored and fine adjusted, by controlling the infiltration ratio of ZnS. On the other hand, ZnS and TiO_2 were infiltrated into SiO_2 opal templates, by atomic vapor deposition [76] (Figure 13). After ZnS:Mn infiltration of a 200 nm sphere SiO_2 opal, the stop band shifted to longer wavelengths, from 434 to 535 nm, due to an increase of the average RI. After etching to form the inverse opal, the reflectance peak shifted to 451 nm, corresponding to the decrease in the average RI. Similar effects were obtained for a 330 nm SiO_2 opal infiltrated with TiO_2, where the reflectivity peak moved to 710 nm as a result of the larger sphere size.

An europium complex, operating as a luminescent probe, has been introduced into monodisperse colloidal silica spheres [93]. The luminescence of the core-shell spheres was dominated by the forced electric dipole transitions ($^5D_0 \rightarrow {}^7F_2$), which are highly sensitive to the environment around the Eu^{3+} ion. The features of this transition, including its intensity, could be altered due to variations in the ligand field and site symmetry of the Eu^{3+} ion. Temperature-dependent decay dynamics indicated that the europium complex in sphere-polymer systems displays higher spontaneous emission rate than free hybrid spheres in air.

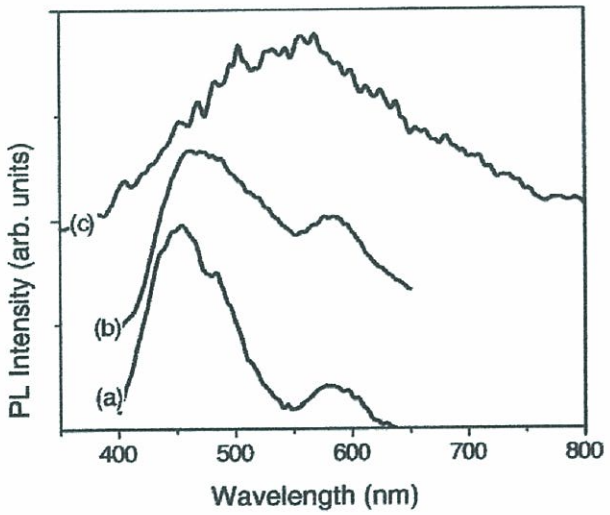

Figure 13. PL spectra excited by a pulsed 337 nm N_2 laser from: (a) 10 nm ZnS:Mn-infiltrated silica opal; (b) TiO_2/ZnS:Mn inverse opal; (c) TiO_2/ZnS:Mn/TiO_2 inverse opal. (Reproduced with permission from ref. [76]).

7.2. Modulation of the refractive index

PCs can be made tunable by filling the structural holes with polymers or liquid crystals, or just by making designs sensitive to the RI change. In 3-D PCs, the optical properties can be tuned through the sphere size. The position of the (111) Bragg diffraction peak shifts linearly toward shorter wavelengths as the sphere diameter decreases, consistent with Bragg's law for normal incidence [94]. Using materials with a strong variation of RI with temperature constitutes another possible method to tune the bandgap [95].

Ferroelectrics represent also an interesting group of materials with high dielectric constant and tunable dielectric properties which vary with external conditions. Thus, a SiO_2 opal template could be infiltrated with a (Ba, Ti) complex alkoxide solution. When the $BaTiO_3$ dopant was fully crystallized, the transmission at the stop band was minimum and its center position reached the longest wavelength at the Curie temperature of the ferroelectric [96].

8. Conclusions

Photonic crystals prepared based on sol-gel processing are an interesting new class of optical materials and structures which can be fabricated by means of relatively simple equipment. This low-cost processing method leads easily to 1-D and 3-D PBG structures. The introduction of defects into 3-D structures and the fabrication of 2-D structures by sol-gel, either planar or fiber-like, still need considerable development. The range of possible applications of PCs, particularly in the fiels of optics and spectroscopy, appear almost endless at present.

9. References

1. H.E. Hinton, D.F. Gibbs, J. Insect. Physiol. 15 (1969) 959.
2. J.V. Sanders, Nature 204 (1964) 1151.
3. E. Yablonovitch, Phys. Rev. Lett. 58 (1987) 2059.
4. S. John, Phys. Rev. Lett. 58 (1987) 2486.
5. E. Yablonovitch, T.J. Gmitter, K.M. Leung, Phys. Rev. Lett. 67 (1991) 2295.
6. E. Ozbay, E. Michel, G. Tuttle, R. Biswas, M.M. Sigalas, K.-M. Ho, Appl. Phys. Lett. 64 (1994) 2059.
7. S.Y. Lin, J.G. Fleming, D.L. Hetherington, B.K. Smith, R. Biswas, K-M. Ho, M.M. Sigalas, W. Zubrzycki, S.R. Kurtz, J. Bur, Nature 394 (1998) 251.
8. A. Blanco, E. Chomski, S. Grabtchak, M. Ibisate, S. John, S.W. Leonard, C. Lopez, F. Meseguer, H. Miguez, J.P. Mondla, G.A. Ozin, O. Toader, H.M. van Driel, Nature 405 (2000) 427.
9. C.J. Brinker, G.W. Scherer, Sol-Gel Science: the physics and chemistry of sol-gel processing. London: Academic Press, 1990.

10. R.M. Almeida, Z. Wang, Proc. SPIE 2002; 4655:24.
11. R.M. Almeida, S. Portal, Curr. Opin. Solid State Mater. Sci. 7 (2003) 151.
12. R.M. Almeida, A.S. Rodrigues, J. Non-Cryst. Solids 326-327 (2003) 405.
13. R.M. Almeida, M.C. Gonçalves, S. Portal, J. Non-Cryst. Solids 345&346 (2004) 562.
14. I.I. Tarhan, M.P. Zinkin, G.H. Watson, Opt. Lett. 20 (1995) 1571.
15. E. Yablonovitch, T.J. Gmitter, R.D. Meade, A.M. Rappe, K.D. Brommer, J.D. Joannopoulous, Phys. Rev. Lett. 67 (1991) 3380.
16. S.V. Gaponenko, A.V. Prokofiev, A.M. Kapitonov, V.N. Bogomolov, A. Eychmuller, A.L. Rogach, JETP Lett. 68 (1998) 142.
17. H. Miguez, C. Lopez, F. Meseguer, A. Blanco, L. Vazquez, R. Mayoral, M. Ocaña, V. Fornés, A. Mifsud, Appl. Phys. Lett. 71 (1997) 1148.
18. D.F. Sievenpiper, M.E. Sickmiller, E. Yablonovitch, Phys. Rev. Lett. 76 (1996) 2480.
19. D.W. McComb, B.M. Treble, C.J. Smith, R.M. De La Rue, N.P. Johnson, J. Mater. Chem. 11 (2001) 142.
20. J.D. Joannopoulos, R.D. Meade, J.N. Winn, Photonic Crystals: Molding the Flow of Light, Princeton University Press, Princeton, 1995.
21. C. Lopez, L. Vazquez, F. Meseguer, R. Mayoral, M. Ocana, H. Miguez, Superlattices Microstruct. 22 (1997) 399.
22. R. Anselmann, H. Winkler, Adv. Eng. Materials 5, 8 (2003) 560.
23. M.A. Kaliteevski, J. Manzanares-Martinez, D. Cassagne, J.P. Albert, Phys. Rev. B 66 (2002) 113101.
24. Handbook of Nanoscience, Engineering and Technology, ed. W.A. Goddart, The electrical engineering series, Boca Raton, CRC Press, 2003.
25. P. Mach, P. Wiltzius, M. Megens, D.A. Weitz, K.H. Lin, T.C. Lubensky, A.G. Yodh, Phys. Rev. E 65 (2002) 031720.
26. A.F. Koenderink, L. Bechger, H.P. Schriemer, A. Lagendijk, W.L. Vos, Phys. Rev. Lett. 88 (2002) 143903.
27. C. López, Adv. Mater. 15 (2003) 1679.
28. F.G. Santamaria, H.T. Miyazaki, A. Urquia, M. Ibisate, M. Belmonte, N. Shinya, F. Meseguer, C. Lopez, Adv. Mater. 14 8 (2002) 1144.
29. S. Noda, K. Tomoda, N. Yamamoto, A. Chutinan, Science 289 (2000) 604.
30. K.M. Ho, C.T. Chan, C.M. Soukoulis, R. Biswas, M. Sigalas, Solid State Commun. 89 (1994) 413.
31. E. Özbay, A. Abeyta, G. Tuttle, M. Tringides, R. Biswas, C.T. Chan, C.M. Soukoulis, K.M. Ho, Phys. Rev. B50 (1994) 1945.
32. A. Chelnokov, S. Rowson, J.M. Lourtioz, L. Duvillaredt, J.L. Coutaz, Electron. Lett. 33 (1997) 1981.
33. A. Feigel, Z. Kotler, B. Sfez, A. Arsh, M. Klebanov, V. Lyubin, Appl. Phys. Lett. 77 (2000) 3221.
34. J.G. Fleming, S.Y. Lin, I. El-Kady, R. Biswas, K.M. Ho, Nature 417 (2002) 52.
35. S.Y. Lin, E. Chow, V. Hietala, P.R. Villeneuve, J.D. Joannopoulos, Science 282 (1998) 274.
36. L. Zavieh, T.S. Mayer, Appl. Phys. Lett. 75 (1999) 2533.

37. I. Divliansky, T.S. Mayer, K.S. Holliday, V.H. Crespi, Appl. Phys. Lett. 82 (2003) 1667.
38. M. Campbell, D.N. Sharp, M.T. Harrison, R.G. Denning, A.J. Turberfield, Nature 404 (2000) 53.
39. H.-B. Sun, S. Matsuo, H. Misawa, Appl. Phys. Lett. 74 (1999) 786.
40. S. Yang, M. Megens, J. Aizenberg, P. Wiltzius, P.M. Chaikin, W.B. Russel, Mater. Chem. 14 (2002) 2831.
41. X. Wang, J.F. Xu, H.M. Su, Z.H. Zeng, Y.L. Chen, H.Z. Wang, Y.K. Pang, W.Y. Tam, Appl. Phys. Lett. 82 (2003) 2212.
42. S. Shoji, S. Kawata, Appl. Phys. Lett. 76 (2000) 2668.
43. E.A. Kamenetzky, L.G. Mangliocco, H.P. Panzer, Science 263 (1994) 207.
44. N.A. Clark, A.J. Hurd, B.J. Ackerson, Nature 281 (1979) 57.
45. H.B. Sunkara, J.M. Jethmalani, W.T. Ford, Chem. Mater. 6 (1994) 362.
46. M. Weissman, H.B. Sunkara, A.S. Tse, S.A. Asher, Science 274 (1996) 959.
47. Z. Cheng, W.B. Russel, P.M. Chalkin, Nature 401 (1999) 893.
48. P.N. Pusey, W. van Megen, Nature 320 (1986) 340.
49. H. Miguez, F. Messeguer, C. Lopez, A. Blanco, J.S. Moya, J. Requena, A. Mifsud, V. Fornes, Adv. Mater. 10 (1997) 480.
50. H. Miguez, F. Meseguer, C. Lopez, A. Mifsud, J. S. Moya, L. Vazquez, Langmuir 13 (1997) 6009.
51. M. Trau, D.A. Saville, I.A. Aksay, Science 272 (1996) 706.
52. R.C. Hayward, D.A. Saville, I.A. Aksay, Nature 404 (2000) 56.
53. M. Holgado, F. Garcia-Santamaria, A. Blanco, M. Ibisate, A. Cintas, H. Miguez, C.J. Serna, C. Molpeceres, J. Requena, A. Mifsud, F. Meseguer, C. Lopez, Langmuir 15 (1999) 4701.
54. W. Wen, N, Wang, H. Ma, Z. Lin, W. Y. Tam, C.T. Chan, P. Sheng, Phys. Rev. Lett. 82 (1999) 4248.
55. A. van Blaaderen, R. de la Rue, P. Wiltzius, Nature 385 (1997) 321.
56. Y. Xia, B. Gates, Y. Yin, Y. Lu, Adv. Mater. 12 (2000) 693.
57. S.H. Park, D. Qin, Y. Xia, Adv. Mater. 10 (1998) 1028.
58. D. Mei, H. Liu, B. Cheng, Z. Li, D. Zhang, P. Dong, Phys. Rev. B58 (1998) 35.
59. P. Jiang, J.F. Bertone, K.S. Hwang, V.L. Colvin, Chem. Mater. 11 (1999) 2132.
60. A.S. Dimitrov, C.D. Dushkin, H. Yosimura, K. Nagayama, Langmuir 10 (1994) 432.
61. N.D. Denkov, O.D. Velev, P.A. Kralchevsky, I.B. Ivanov, H. Yoshimura, K. Nagayama, Nature 361 (1999) 26.
62. Z.Z. Gu, A. Fujishima, O. Sato, Chem. Mater. 14 (2002) 760.
63. Y.A Vlasov, X.Z. Bo, J.C. Sturm, D.J. Norris, Nature 414 (2001) 289.
64. V. Kozhukharov, C. Trapalis, B. Samuneva, E. Kirilova, J. Mater. Sci. Lett. 11 (1992) 1206.
65. C.C.Trapalis, M.A. Karakassides, G. Kordas, X. Aslanoglou, Mater. Lett. 25 (1995) 265.
66. J. Belessa, S. Rabaste, J.C. Plenet, J. Dumas, J. Mugnier, O. Marty, Appl. Phys. Lett. 79 (2001) 2142.

67. S. Rabaste, J. Bellessa, A. Brioude, C. Bovier, J.C. Plenet, R. Brenier, O. Marty, J. Mugnier, J. Dumas, Thin Solid Films 416 (2002) 242.
68. P.K. Biswas, D. Kundu, D. Ganguli, J. Mater. Sci. Lett. 6 (1987) 1481.
69. D. Kundu, P.K. Biswas, D. Ganguli, J. Non-Cryst. Solids 110 (1989) 13.
70. K.M. Chen, A.W. Sparks, H-C. Luan, D.R. Lim, K. Wada, L.C. Kimerling, Appl. Phys. Lett. 75 (1999) 3805.
71. Q. Zhang, X. Li, J. Shen, G. Wu, J. Wang, L. Chen, Mater. Lett. 45 (2000) 311.
72. H. Miguez, A. Blanco, C. Lopez, F. Meseguer, H.M. Yates, M.E. Pemble, F. Lopez-Tejeira, F.J. Garcia-Vidal, J. Sanchez-Dehesa, J. Lightwave Technol. 17 (1999) 1975.
73. J.D. Joannopoulos, Nature 414 (2001) 257.
74. Handbook of Chemistry and Physics, CRC Press, 61st Edition.
75. P.W. Atkins, Physical Chemistry, Oxford University Press, 6th ed. 2000, p.154.
76. J.S. King, D. Heineman, E. Graugnard, C.J. Summers, Appl. Surf. Science (2005) (in press).
77. A. Imhof, D.J. Pine, Nature 389 (1997) 948.
78. V. N. Astratov, A.M. Adawi, S. Fricker, M.S. Skolnick, D.M. Whittaker, P.N. Pusey, Phys. Rev.B 66 (2002) 165215.
79. Z.Y. Li, Z.Q. Zhang, Phys. Rev. B62 (2000) 1516.
80. Z.Y. Li, Z.Q. Zhang, Adv. Mater. 13 (2001) 2001.
81. K. Wostyn, Y.X. Zhao, G. de Schaetzen, L. Hellemans, N. Matsuda, K. Clays, A. Persoons, Langmuir 19 (2003) 4465.
82. E. Palacios-Lidon, J.F. Galisteo-Lopez, B.H. Juarez, C. Lopez, Adv. Mater. 16 (2004) 341.
83. J.F. Galisteo-López, F. García-Santamaría, D. Golmayo, B.H. Juárez, C. López, E. Palacios-Lidón, Photonics and Nanostructures – Fundamentals and Applications 2 (2004) 117.
84. B. Gates, Y. Xia, Appl. Phys. Lett. 78 (2001) 3178.
85. W. Lee, S.A. Pruzinsky, P.V. Braun, Adv. Mater. 14 (2002) 271.
86. A. van Blaaderen, R. Ruel, P. Wiltzius, Nature 385 (1997) 321.
87. Y.D. Yin, Y.N. Xia, Adv. Mater. 14 (2002) 605.
88. R.M. Almeida, A.C. Marques and S. Portal, Optical Materials (2005) (in press).
89. A. Blanco, C. Lopez, R. Mayoral, H. Migues, F. Meseguer, A. Mifsud, J. Herrero, Appl. Phys. Lett. 73 (1998) 1781.
90. S.G. Romanov, T. Maka, C.M. Sotomayor Torres, M. Muller, R. Zentel, Appl. Phys. Lett. 79 (2001) 731.
91. A. Blanco, H. Miguez, F. Meseguer, C. Lopez, F. Lopez-Tejeira, J. Sanchez-Dehesa, Appl. Phys. Lett. 78 (2001) 3181.
92. X. Chang, J. Cao, H. Ji, B. Fang, J. Feng, L. Pan, F. Zhang, H. Wang, Materials Chem. Phys. 89 (2005) 6.
93. D.Zhao, W. Qin, J. Zhang. C. Wu, G. Qin, G. De, J. Zhang, S. Lü, Chemical Physics Letters 403 (2005) 129.
94. H. Miguez, A. Blanco, C. López, F. Meseguer, H.M. Yates, M.E. Pemble, F. López-Tejeira, F.J. García-Vidal, J. Sánchez-Dehesa, J. Lightwave Technol. 17 N11 (1999) 1975.

95. R.T. Bise, R.S. Windeler, K.S. Kranz, C. Kerbage, B.J. Eggleton, D.J. Trevor, in: OSA Trends in optics and photonics, optical fiber communications conference technical digest, vol. 70, Washington, DC: Optical Society of America; 2002, p. 466.
96. C.-H. Kuo, Z. Ye, Phys. Letters A 331 (2004) 342.